Computer Simulation of Nanometric Optical Waveguide Circuits using Surface Plasmon Polariton

Kazuo Tanaka, Masahiro Tanaka, and Tatsuhiko Sugiyama
Department of Electronics and Computer Engineering, Gifu University, Yanagido 1-1, Gifu City, Japan 501-1193

1. Introduction

Recently, many researchers are much interested in the construction of optical circuits on subwavelength or nanometric scales [1]-[5]. The size and density of optical devices employing conventional dielectric optical waveguide and photonic crystals will in principle be limited by the diffraction limit of light. In contrast, optical waveguides based on surface plasmon polaritons (SPPs) can be miniaturized much further, leading to the possible development of nanometric optical circuits. The present authors recently proposed an SPP gap waveguide (SPGW) as a basic element of nanometric optical circuits [6]-[8]. The waveguide mechanism of the SPGW is derives from the low phase velocity exhibited by SPPs in nanometrically narrow gap regions between two parallel metal substrates compared to that in wide gap regions. In this paper, the computer simulations of practical nanometric *H*-plane and *E*-plane optical waveguide circuits based on SPGWs are demonstrated through three-dimensional volume integral eqautoion.

2. Volume integral equation

The scattering problem for the metallic structure in this paper is solved using a volume integral equation, as given by [9]

$$\boldsymbol{E}^{i}(\boldsymbol{x}) = \boldsymbol{D}(\boldsymbol{x})/\varepsilon_r(\boldsymbol{x}) - (k_0^2 + \nabla\nabla\bullet)\boldsymbol{A}(\boldsymbol{x}) \tag{1}$$

where $k_0 = \omega/c$ (c is light velocity in free space, ω is angular frequency), $\boldsymbol{D}(\mathbf{x})$ is the total electric flux, $\boldsymbol{E}^{i}(\mathbf{x})$ is the incident electric field, and $\boldsymbol{A}(\boldsymbol{x})$ is the vector potential, which is expressed by the following volume integral:

$$\boldsymbol{A}(\boldsymbol{x}) = (1/\varepsilon_0)\iiint_V \{[\varepsilon_r(\boldsymbol{x}') - \varepsilon_0]/\varepsilon_r(\boldsymbol{x}')\} G(\boldsymbol{x}\mid\boldsymbol{x}')\boldsymbol{D}(\boldsymbol{x}')dv'\cdot \tag{2}$$

Here, $g(\mathbf{x}|\mathbf{x}')$ is a free-space Green's function given by

$$G(\boldsymbol{x}\mid\boldsymbol{x}') = \exp(-jk_0|\boldsymbol{x}-\boldsymbol{x}'|)/(4\pi|\boldsymbol{x}-\boldsymbol{x}'|)\cdot \tag{3}$$

The volume integral region V in (2) represents the entire space, and $\varepsilon_r(\boldsymbol{x})$ represents the distribution of permittivity, where $\varepsilon_r(\boldsymbol{x}) = \varepsilon_1$ in the metal and $\varepsilon_r(\boldsymbol{x}) = \varepsilon_0$ in the void space, where ε_0 is the permittivity in a vacuum. When the region in which $\varepsilon_r(\boldsymbol{x}') - \varepsilon_0$ is nonzero is finite, the integral region V has finite volume. In this case, it is possible to solve (1) numerically by the well-established method of moments. To obtain the solution, the entire region of the circuit is divided into small discretized cubes of size $\delta\times\delta\times\delta$, and (1) and (2) are discretized by the method of moments using roof-top functions as basis and testing functions. The resultant system of linear equations is then solved by iteration using the generalized minimized residual method (GMRES) with fast Fourier transformation (FFT) [9], [10]. The validity of the code was checked by confirming that the code gives a reasonably accurate solution compared to the rigorous solution for a dielectric sphere.

3. Nanometric *H*-plane optical waveguide circuits

The operating wavelength considered in this analysis is $\lambda = 573$ nm, the metal supporting the SPP is assumed to be silver with a relative permittivity of $\varepsilon_1/\varepsilon_0 = -12.4 - j0.85$. A schematic of the *H*-plane planar optical SPGW circuits considered here is shown in Fig. 1. A square hole of dimensions $C_x \times C_y \times C_z$ is bored into the metallic substrate such that the hole is surrounded by four walls and one bottom plate. The walls and bottom plate are assumed to be thicker than the optical skin-depth of the metal, defined as d in Fig. 1. Inside the square hole, the ridge structure is preserved, forming a four-port asymmetric branching circuit as shown by dotted curves in the *x*-*y* plane. A cover plate of thickness d is then placed over the hole, creating a small gap between the ridge and the cover plate. The width of the ridge is given by w and the gap between the ridge and the cover plate is given by g. Since the phase velocity of the SPP in the gap region is smaller than that in the surrounding region in the hole, the gap between the ridge and the cover plate constitutes an SPGW and optical waves are expected to be guided along the ridge structure in the *x*-*y* plane, i.e., constituting a four-port branching circuit. A plane wave of a

unit amplitude (i.e., $|\boldsymbol{E}^{\mathrm{i}}|^2 = 1$) is assumed to be incident from the negative x direction on an entrance hole with a cross-section shown in Fig. 1, exciting the SPPs in the SPGW inside the circuit. The entrance hole is also a SPGW, and the SPP excited within is confined in the narrow-gap region in the hole. The SPP excited in the entrance hole is incident on the port (I) of the branching SPGW circuit. The output ports (II), (III) and (IV) of the branching SPGW are closed off by metallic walls. To ensure that the field in the entrance hole is the guided mode only, the incident vector is set to be rotated by $\pi/4$ with respect to the positive y axis to achieve oblique incidence to the entrance hole. The parameters used in the branching circuit shown in Fig. 1 are given as follows. Circuit size: $k_0C_x = 5.5$, $k_0C_y = 5.4$, $k_0C_z = 1.2$, $k_0d = 1.0$, $k_0l_x = 2.8$, $k_0l_y = 3.7$, $k_0b_1 = 0.8$, $k_0b_2 = 2.0$, $k_0h = k_0(C_z - g) = 1.0$. Cross-section of SPGWs: $k_0w = 0.2$, $k_0g = 0.2$. Cross-section of entrance hole: $k_0a_y = k_0a_z = 0.2$, $k_0b_y = 1.8$, $k_0b_z = 0.4$. Discretized cube: $k_0\delta = 0.05$. The overall effective dimensions of the optical circuits are therefore approximately $0.88\lambda \times 0.86\lambda \times 0.51\lambda$. The optical scattering problem is solved for the complex structure shown in Fig. 1 using (1) to obtain the optical field inside the circuit. The dependence of the waveguide characteristics on gap width g in Fig. 1 is shown in Fig. 2. Fig. 2 shows total optical intensity $|\boldsymbol{E}|^2$ on the plane parallel to the x-y plane and located at a distance $k_0\xi = 0.025$ from the ridge in the gap region. Standing waves can be clearly seen to arise along the ridge structures in the circuit. Notice that the intensity scale normalized by the incident intensity of these results is 0–20. The intensity is enhanced by the plasmon enhancement. The approximate values of $\mathrm{Re}(k_w/k_0)$ calculated from the distances between standing wave maximum (SWMs) are $\mathrm{Re}(k_w/k_0) \approx 1.95$, 2.2 and 3.0 for $k_0g = 0.3$, 0.2 and 0.1, respectively. The larger the gap width, the smaller the value of $\mathrm{Re}(k_w/k_0)$ (larger wavelength) for the guided SPPs. We can clearly see that the optical fields are guided along the ridge structure as designed in Figs. 2(b) and 2(c).

3. Nanometric *E*-plane optical waveguide circuits

A schematic of the *E*-plane optical circular bend circuits with SPGWs considered here is shown in

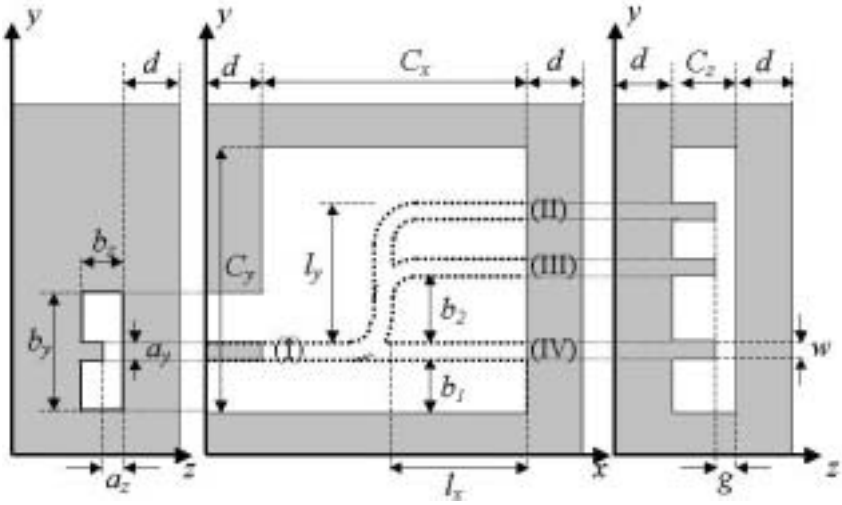

Fig. 1 Schematic of an subwavelength-scale H-plane planar circuit.

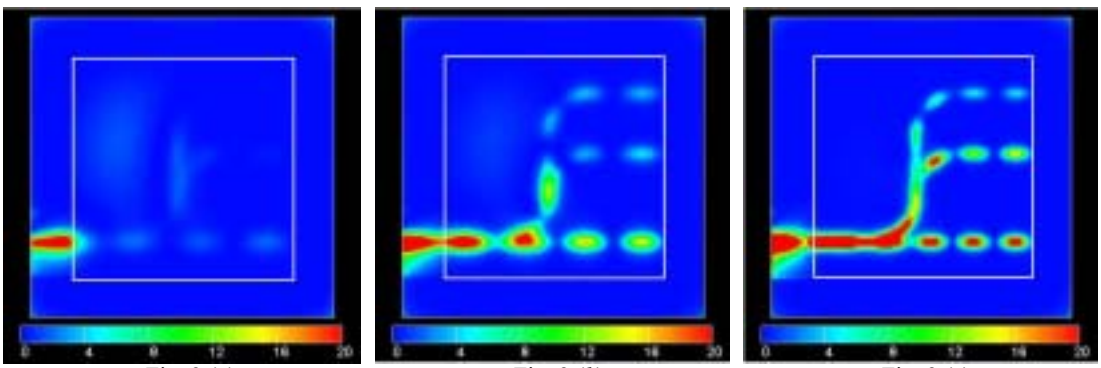

Fig. 2 (*a*) Fig. 2 (*b*) Fig. 2 (*c*)

Fig. 2 Optical intensities for (a) $k_0g = 0.3$ (b), (b) $k_0g = 0.2$ and (c) $k_0g = 0.1$. White rectangle indicates the region $C_x \times C_y$ in Fig. 1.

Fig. 3. The silver substrate has dimensions of $l_x \times l_y \times l_z$. The cross-section of the waveguide has an "I" shape, with wide gap region of dimensions $b_x \times b_y$ and narrow gap region of $a_x \times a_y$. The space inside the SPGW is connected to the upper free space through the truncated upper wide gap region of the SPGW. The phase velocity of the SPP in the narrow gap region is lower than that in the wide gap region, including free space. The free space region with permittivity of ε_0 above the silver substrate is bounded by five metallic plates with thickness d and relative permittivity of $\varepsilon_2/\varepsilon_0 = -12.4 - j30.85$, as shown in the figure. Without the cover over the substrate, it proved to be difficult to discriminate the guided field in the SPGWs from the field excited by the diffracted incident wave. The void space inside the SPGWs is assumed to be free space with permittivity of ε_0 in this analysis. The E-plane bend circuit using SPGWs consists of a short straight section with length w_y, a bend section with average radius R, and a long straight section with length w_x, as shown in Fig. 3. A plane wave is assumed to be incidence normal to the "I" shaped entrance aperture [11] (x-z plane) formed in the substrate and cover from the negative y direction. In order to excite the SPP inside the waveguide, the incident electric field must be oriented in the x direction. The excited SPP in the short straight section is transmitted to the long straight section through the bend section. The exits of the long straight sections of the SPGWs are closed in order to prevent the introduction of a diffracted incident wave from the ends of the waveguide. The long straight section is made sufficiently long to ensure that the end of the waveguide is connected to the matched terminal, that is, to ensure negligibly small reflection from the end of the waveguide. The parameters used in the model bend circuit were as follows. Circuit size: $k_0l_x = 50.0$, $k_0l_y = 12.0$, $k_0l_z = 2.8$, $k_0w_y = 4.0$, and $k_0D = 1.0$. Cross-section of o-SPGWs: $k_0a_x = k_0a_z = 0.4$, $k_0b_x = 0.8$, $k_0b_z = 1.4$. Cover: $k_0C_z = 9.2$ and $k_0d = 1.0$. Discretized cube: $k_0\delta = 0.1$. The overall dimensions of the optical circuits with the cover are approximately $8.0\lambda \times 2.0\lambda \times 1.9\lambda$. In order to position the region of strong optical intensity as near the surface of the circuit as possible, k_0b_z' shown in Fig. 1 was set to 0 in this treatment.

The electric field distribution of the circuits shown can be obtained by solving (1) numerically. The distributions of total optical intensity $|\boldsymbol{E}|^2$ for the case of a unit intensity incident field (i.e., $|\boldsymbol{E}^i|^2 = 1$) are shown in Fig. 4 on a plane parallel to the x-y plane indicated by (B) in Fig. 1 for $k_0R = 0.4$, 2.2, and 6.2. The distance between this plane and the surface of the circuit is given by $k_0h_1 = 0.15$ shown in Fig. 3. Since the optical intensity larger than 50 times of the incident intensity is truncated in Fig. 4, the maximum optical intensity in Fig. 3 is 50. Enhanced optical intensities occur in the narrow gap region of the SPGWs, demonstrating that the optical waves are confined and guided along the bend circuit. We can observe sharp peaks in the optical intensities shown in Fig. 4. They are due to the enhanced fields near the edge of the small cubes generating in the discretization of the bend. The free-space region surrounded by the metallic cover above the substrate is sufficiently large to admit radiation from the bend-section. In order to know the radiation fields into the free space region inside the cover, the intensity distribution on a plane parallel to the y-z plane indicated by the white dotted line in Fig. 4(a) are shown in Fig. 5. We can observe the strong and confined guided waves and weak standing wave due to the radiated SPPs in Fig. 5.

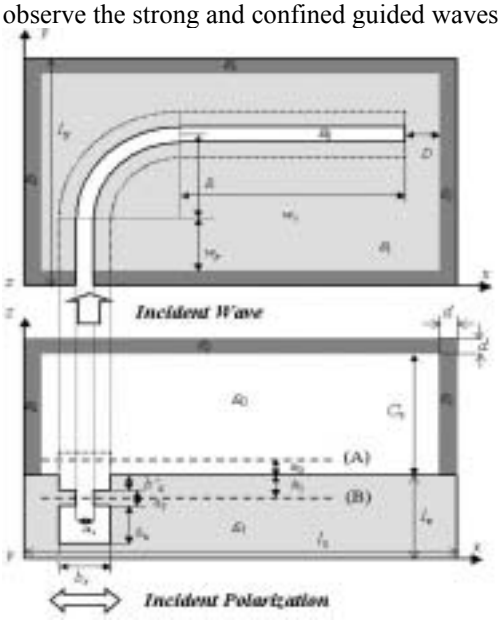

Fig. 3 Schematic of bend-circuit with SPGWs.

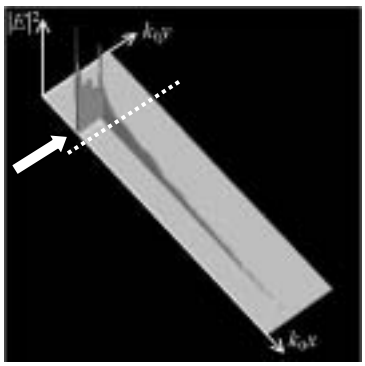

Fig. 4 (a)

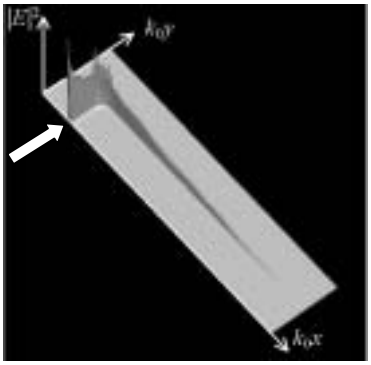

Fig. 4 (b)

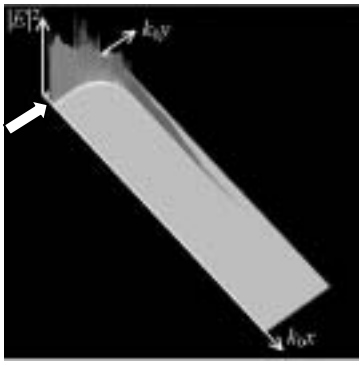

Fig. 4 (c)

Fig. 4. Distributions of optical intensity on the plane (B) in Fig. 1 for average radii k_0R of (a) 0.4, (b) 2.2, and (c) 6.2. The range is given by $0 < k_0x < 50$ and $0 < k_0y < 12$. Maximum value is 50 times of the incident intensity. White arrows show positions of entrance aperture.

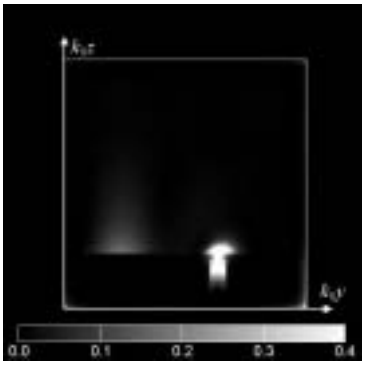

Fig. 5. Distribution of optical intensity on the plane parallel to y-z plane indicated by a white line in Fig. 3. Maximum value is 0.4 times of the incident intensity.

We looked for the radiation field in the free space region inside the cover in the simulation results. However, no optical intensity distribution that could be related to the radiation field was observed in the free-space region inside the cover. These simulations show that the optical field is confined in the narrow gap region and indicate the smallness of radiation fields. Thus, the radiation field around the bend structure can be considered to be very minor in the *E*-plane circuits.

3. Conclusions

The feasibility of constructing nanometric optical circuits through the use of surface plasmon polariton gap waveguides (SPGWs) was investigated by three-dimensional simulations using a volume integral equation. The *H*-plane and *E*-plane planar branching waveguide circuits were considered. The nanometric optical circuits using SPGWs simulated in this paper can fulfill the basic function designed. It is possible to control the phase velocities of SPPs by the gap-width in nanoscale SPGWs. This technique may be widely applied to nanometric optical devices. It would be of great interest to know how to improve all the circuit characteristics by changing geometrical parameters, material constants and wavelength.

References

[1] J. Takahara, S. Yamagishi, H. Taki, A. Morimoto and T. Kobayashi, "Guiding of a one-dimensional optical beam with nanometer diameter", Opt. Lett., **22** 4765-477 (1997).

[2] S. A. Maier, M. L. Brongersma, P. G. Kik, S. Meltzer, A. A. G. Requicha, H. A. Atwater, "Plasmonics - A route to nanoscale optical devices", Adv. Mat. **13**, 1501-1505 (2001).

[3] T. Yatsui, M. Kourogi, and M. Ohtsu, **"**Plasmon waveguide for optical far/near-field conversion"**,** Appl. Phys. Lett. **79**, 4583-4585 (2001).

[4] T. Goto, Y. Katagiri, H. Fukuda, H. Shinojima, Y. Nakano, I. Kobayashi, Y. Mitsuoka, "Propagation loss measurement for surface plasmon-polariton modes at metal waveguides on semiconductor substrates", Appl. Phys. Lett. **84**, 852-854 (2004).

[5] H. Ditlbacher, J. R. Krenn, G. Schider, A. Leitner, F. R. Aussenegg, "Two-dimensional optics with surface plasmon polaritons", Appl. Phys. Lett. **81**, 1753-1755 (2002).

[6] K. Tanaka and M. Tanaka, "Simulations of nanometric optical circuits based on surface plasmon polariton gap waveguide", Appl. Phys. Lett. **82**, 1158-1160 (2003).

[7] K. Tanaka and M. Tanaka, "Simulations of nanometric optical circuits: Open-type surface plasmon polariton gap waveguide", Jpn. J. Appl. Phys. **42**, L585 - L588 (2003).

[8] K. Tanaka, M. Tanaka and T. Sugiyama, "Simulation of practical nanometric optical circuits based on surface plasmon polariton gap waveguide", Optics Express **13**, 256-266 (2005).

[9] P. Zwamborn and P. M. van den Berg, "The three-dimensional weak form of the conjugate gradient FFT method for solving scattering problems", IEEE Trans on **MTT-40**, No. 9, 1757-1766 (1992).

[10] R. Barrett, M. Berry, T. F. Chan, J. Demmel, J. Donato, J. Dongarra, V. Eijkhout, R. Pozo, C. Romine and H. van der Vorst, *Templates for the Solution of Linear Systems: Building Blocks for Iterative Methods*, Society for Industrial and Applied Mathematics (1994).

[11] 13. Kazuo Tanaka and Masahiro Tanaka, Simulation of an aperture in the thick metallic screen that gives high intensity and small spot size using surface plasmon polariton", *Journal of Microscopy*, **210**, 294-300 (2003).